Comparative energy and exergy analysis of a novel three-fluid condensing heat exchanger applied to industrial gas boilers and high-moisture drying processes

Marcel Barzantny[a], *Wojciech Kostowski*[b], *Michał Majchrzyk*[c], *Piotr Ostrowski*[d], *Ion Dosa*[d]

[a] *Silesian University of Technology, Gliwice, Poland, marcel.barzantny@polsl.pl CA*
[b] *Silesian University of Technology, Gliwice, Poland, wojciech.kostowski@polsl.pl*
[c] *Silesian University of Technology, Gliwice, Poland, michal.majchrzyk@polsl.pl*
[d] *Silesian University of Technology, Gliwice, Poland, piotr.ostrowski@polsl.pl*
[e] *University of Petrosani, Petrosani, Romania, IonDosa@upet.ro*

Abstract:
The transition towards highly efficient industrial thermal systems requires the implementation of low temperature waste heat recovery (LTWHR) technologies, particularly focusing on latent heat extraction from exhaust gases. Conventional heat exchangers often face limitations in sub-dew point operations due to corrosion risks and the lack of low-temperature heat sinks. This study proposes and evaluates a novel, modular three-fluid heat and mass exchanger (H3XA) designed for simultaneous deep waste heat recovery, oxidizer preheating, and optional third-medium injection for wet exhaust gas cleaning. To assess the thermodynamic feasibility and system-level benefits of the proposed architecture, a comparative energy and exergy analysis is conducted across two distinct industrial applications: a standard natural gas-fired boiler and a high-moisture industrial drying process. A proprietary 1D analytical model, utilizing the Chilton-Colburn analogy for simultaneous heat and mass transfer, is employed to simulate the heat exchanger's performance under varying inlet conditions. The generated performance data is subsequently used to formulate extended exergy balances for both systems. The parametric study investigates the impact of flue gas temperature and moisture content on the overall energy efficiency and exergy destruction within the systems. Preliminary results indicate that while the application of the H3XA module significantly improves the energy efficiency of standard gas boilers through combustion air preheating, its integration into high-moisture drying processes yields an even higher reduction in exergy destruction due to the massive potential for latent heat recovery. The findings demonstrate that the three-fluid architecture serves as a versatile and highly effective platform for advancing decarbonization in diverse industrial sectors.

Keywords:
Plate heat exchanger, Waste heat recovery, Condensation, Decarbonisation

1. Introduction

The ongoing energy transition process in Europe, which encompasses power generation, district heating, and various industrial sectors, sets a series of ambitious goals, notably achieving climate neutrality by 2050. Achieving these goals remains challenging for fossil-fuel-reliant economies like Poland, necessitating the deployment of highly efficient bridge technologies. In this context, any manageable waste heat is considered a valuable resource, aligning with the principle that 'energy efficiency is the 1st fuel'.

Waste heat recovery (WHR) involves capturing and reusing heat generated in industrial processes that would otherwise be lost to the environment [1]. Globally, it is estimated that approximately 70% of the chemical energy released in combustion processes is lost during subsequent thermodynamic conversions [2]. Consequently, the implementation of deep WHR technologies is essential to minimize

economic and environmental costs. The critical need for improved energy efficiency is underscored by several strategic frameworks at both the global and national levels:

- Sustainable Energy for All (SE4All): Launched by the UN, aiming to double the global rate of improvement in energy efficiency by 2030 [3].
- Energy Efficiency Directive (EU/2023/1791): Establishes the 'energy efficiency first' principle as a fundamental pillar of EU energy policy [4].
- UAE Consensus at COP28: Represents a commitment by nearly 120 countries to double global energy efficiency by 2030 [5].
- Energy Policy of Poland until 2040 (PEP2040): Outlines the strategic direction for Poland's energy transition, heavily emphasizing enhanced energy efficiency across multiple sectors [6].

Despite these clear directives, existing WHR systems often exhibit overlooked limitations that restrict their effectiveness. Low-temperature waste heat recovery (LTWHR), defined as recovering heat from sources below 100°C [7], poses a major technological challenge. Conventional systems are typically constrained by the threat of corrosion, forcing operators to maintain exhaust gas temperatures well above the dew point (typically 120–140°C) to prevent the condensation of acidic compounds [8, 9]. This standard practice unintentionally wastes the massive latent heat potential trapped within exhaust moisture, particularly in high-moisture applications like industrial drying or the combustion of hydrogen-rich fuels, such as natural gas.

Furthermore, traditional structural approaches to heat exchangers (HE) struggle in sub-dew point environments. Tubular heat exchangers (THEs), while robust for high-temperature applications, require complex manufacturing and often suffer from severe scaling when water is used as the heat-receiving medium [10, 11]. Conversely, Plate Heat Exchangers (PHE) offer a highly compact, lightweight, and modular alternative [12, 13]. However, existing literature indicates a significant knowledge gap regarding the optimization of gas-to-gas PHEs designed specifically to handle simultaneous heat and mass transfer (condensation) in corrosive environments [14, 15].

To unlock the full thermodynamic potential of LTWHR, it is necessary to move beyond simple sensible heat recovery and implement condensing systems [16, 17]. Utilizing counter-current flow arrangements, which provide the highest thermal effectiveness [18, 19], such systems can deeply cool exhaust gasses. Because traditional low-temperature liquid sinks are often unavailable [20, 21], combustion air preheating serves as an optimal heat sink. However, deep condensation introduces a secondary challenge: trapping particulates in water droplets, which can cause equipment clogging. This can be mitigated through external fluid injection [22–24], which actively cleans the exhaust gas while augmenting heat transfer, essentially laying the groundwork for integrated ecological waste heat recovery (EWHR) [25, 26].

While energy (First Law) analyses show the bulk improvements of such systems, they fail to distinguish between the quality of the thermal energy recovered. Exergy (Second Law) analysis is therefore required to accurately assess the reduction in thermodynamic irreversibility, particularly when comparing fundamentally different thermal processes. The primary objective of this study is to propose and thermodynamically evaluate a novel, modular three-fluid heat and mass exchanger (H3XA), Figure 1 based on the idea of Ostrowski [27]. This architecture is specifically designed for simultaneous deep waste heat recovery, oxidizer preheating, and optional third-medium injection for wet exhaust gas cleaning. To assess its thermodynamic feasibility, a comparative energy and exergy analysis is conducted across two distinct industrial sectors characterized by unexploited potential: a standard natural gas-fired boiler and a high-moisture industrial drying process. Utilizing a proprietary 1D analytical model based on the Chilton-Colburn analogy for simultaneous heat and mass transfer, this paper investigates the impact of flue gas temperature, moisture content, and third-fluid injection rates on overall energy efficiency and system exergy destruction. Ultimately, this research aims to demonstrate that a three-fluid condensing architecture serves as a highly effective platform for advancing decarbonization in complex industrial environments.

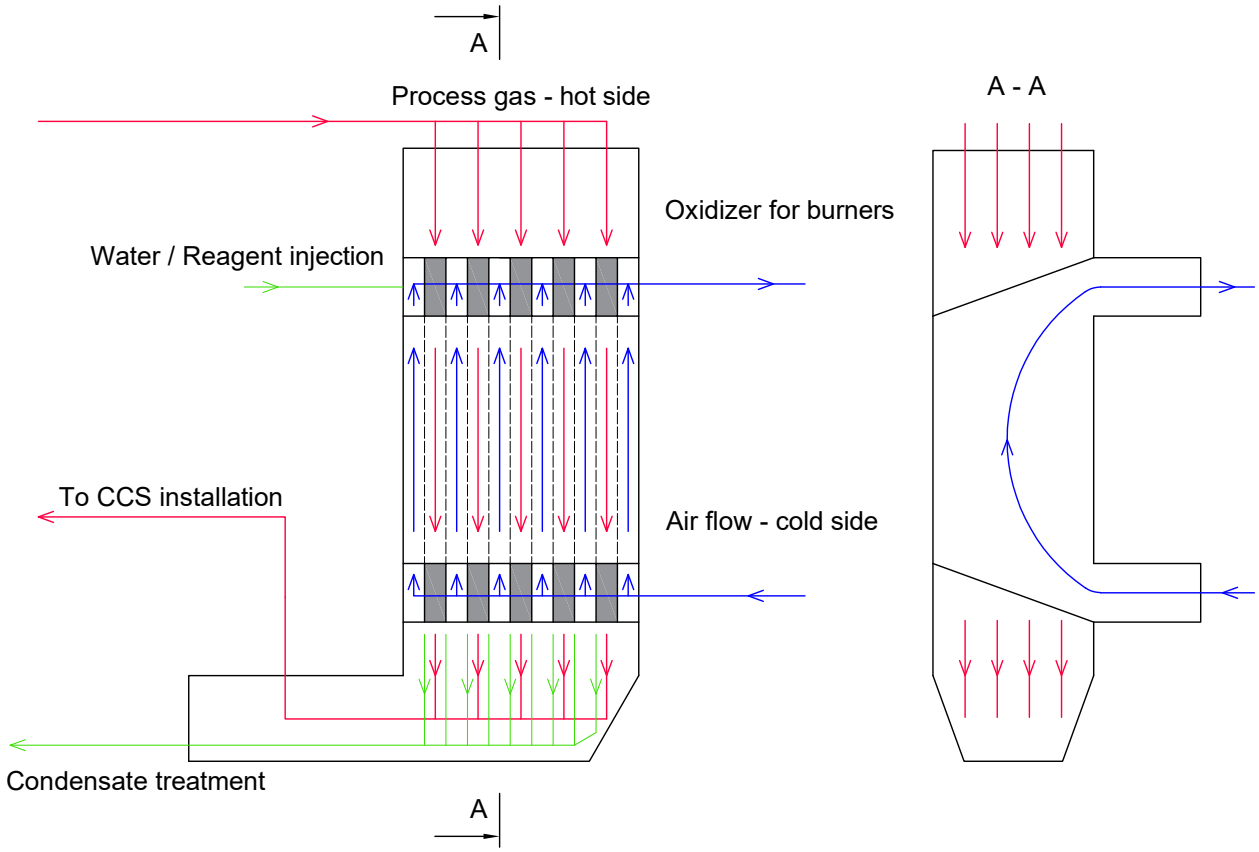

Figure 1: Working principle of the proposed PHE design with described possible further processing ways of the waste streams such as providing oxidizer for burners, cooperating with CCS installations and sewage treatment of the condensate.

2. Methodology

To quantitatively assess the thermodynamic performance of the proposed three-fluid heat and mass exchanger (H3XA) and its impact on the overall industrial systems, a comprehensive calculation algorithm was developed. The evaluation is divided into two fundamental levels: the component-level heat and mass transfer analysis of the H3XA module and the system-level energy and exergy balances of the integrated industrial plants.

2.1. Component-level heat and mass transfer model

The thermal performance of the condensing heat exchanger was evaluated by discretising the heat transfer surface into a series of sequential segments. Within each segment, the total heat transfer rate (Q_{tot}) is partitioned into sensible (Q_{sens}) and latent (Q_{lat}) components. To ensure strict thermodynamic consistency and prevent non-physical temperature crossovers, the maximum possible heat transfer for a given segment is bounded using the Effectiveness-NTU (ε-NTU) method, expressed as:

$$Q_{tot} = \varepsilon C_{min}(T_{h,in} - T_{c,in}) \tag{1}$$

where ε is the segment effectiveness, C_{min} is the minimum heat capacity rate between the streams, and $T_{h,in}$ and $T_{c,in}$ represent the inlet temperatures of the hot and cold streams for the respective segment.

The mass transfer rate of water vapour condensing on the heat exchanger surface ($\dot{m}_{cond}$) is initially determined using the Colburn analogy. The driving force for this process is the local partial pressure gradient, calculated as:

$$\dot{m}_{cond} = K_g A_{cell}(p_{v,bulk} - p_{v,int}) \tag{2}$$

where K_g is the local mass transfer coefficient, A_{cell} is the heat transfer area of the segment, whilst $p_{v,bulk}$ and $p_{v,int}$ denote the partial pressures of water vapour in the bulk gas stream and at the condensate film interface, respectively.
Crucially, under conditions of thermal capacity mismatch, where the kinetic potential for condensation exceeds the sensible cooling capacity of the secondary air stream, the actual condensation rate is energetically constrained. To maintain adherence to the First Law of Thermodynamics, the latent heat component is dynamically reconciled with the available heat sink capacity:

$$Q_{lat} = Q_{tot} - Q_{sens} \tag{3}$$

$$\dot{m}_{actual} = \frac{Q_{lat}}{h_{fg}} \tag{4}$$

where h_{fg} is the enthalpy of vaporisation. This energy-bound correction ensures that the mass transfer strictly corresponds to the physical cooling capacity of the cold air stream, thereby ensuring global energy conservation across the heat exchanger.

2.2. System-level exergy analysis framework

To evaluate the true thermodynamic quality of the recovered thermal energy, an extended exergy analysis was implemented. The dead state was defined consistently at $T_0 = 293.15\text{K}$ and $p_0 = 101325\text{Pa}$.
The specific physical exergy b for any given state was calculated using the fundamental relation:

$$b = (h - h_0) - T_0 (s - s_0) \tag{5}$$

where h_0 and s_0 are the specific enthalpy and specific entropy evaluated at the dead state. While these properties were evaluated as a standard mixture for the cold oxidiser stream, the hot exhaust gas required a more rigorous approach to accurately capture the thermodynamics of condensation. As water vapour undergoes phase change, the molar composition of the remaining gas mixture continuously shifts. Consequently, the specific properties h and s of the exhaust gas were evaluated dynamically using real-fluid property databases (CoolProp), recalculating the properties based on the updated partial pressures of the constituent gases at the respective inlet and outlet states.
The exergy rate of each thermodynamic stream crossing the system boundaries was defined as $\dot{B} = \dot{m}b$. To ensure a strict balance during sub-dew point operation, the exergy carried away by the liquid water must be explicitly isolated. The net exergy extracted from the hot stream is thus defined as:

$$\Delta\dot{B}_{\text{extracted}} = \dot{B}_{h,\text{in}} - \dot{B}_{h,\text{out}} - \dot{B}_{\text{cond}} \tag{6}$$

where $\dot{B}_{\text{cond}}$ represents the physical exergy rate of the drained liquid condensate.
The irreversibility inherent to the simultaneous heat and mass transfer within the H3XA module is quantified via the absolute exergy destruction rate $\delta\dot{B}_D$. Utilising the Gouy-Stodola theorem, this was calculated directly from the total entropy generation, explicitly accounting for both the gaseous and liquid effluent streams:

$$\delta\dot{B}_D = T_0 \left(\sum (\dot{m}s)_{\text{out}} - \sum (\dot{m}s)_{\text{in}} \right) \tag{7}$$

The general form of the exergy balance for the entire thermal system follows the standard definition:

$$\dot{B}_F = \dot{B}_P + \delta\dot{B}_L + \delta\dot{B}_D \tag{8}$$

where $\dot{B}_F$ is the exergy of the fuel, $\dot{B}_P$ is the exergy of the useful product, and $\delta\dot{B}_L$ represents external exergy losses. For the gaseous fuel utilised in the system, the chemical exergy $\dot{B}_F$ is approximated using the empirical ratio α for natural gas ($\alpha \approx 1.04$) applied to the lower heating value H_u:

$$\dot{B}_F = \dot{m}_f \alpha H_u \tag{9}$$

2.3. Scenario-specific formulations

To demonstrate the versatility of the H3XA module, the computational framework was applied to two distinct boundary scenarios. The baseline scenario involves sensible heat exchange, whereas the secondary scenario explores complex, moisture-driven latent heat recovery.

Industrial gas boiler

This baseline scenario represents a standard natural gas-fired boiler with a nominal thermal capacity of 500 kW ($\dot{Q}_{\text{nom}} = 500\,\text{kW}$). The formulation of energy and exergy balances in this application is relatively straightforward. The primary functional requirement is limited to the sensible heating of a working fluid, and the product exergy $\dot{B}_P$ is strictly defined by the thermal energy transferred to the boiler feedwater. Based on the nominal thermal power and the specific heat capacity of water $c_{p,w}$, the product exergy is:

$$\dot{B}_P = \dot{Q}_{\text{nom}} - \dot{m}_w c_{p,w} T_0 \ln\left(\frac{T_{w,\text{out}}}{T_{w,\text{in}}}\right) \tag{10}$$

The integration of the H3XA module reduces the required fuel exergy input ($\dot{B}_F$) by pre-heating the combustion air, thereby directly improving the overall exergy efficiency $\eta_{\text{sys}} = \dot{B}_P/\dot{B}_F$.

High-moisture industrial dryer

To ensure a direct comparative analysis of the module's capacity for deep latent heat recovery, this scenario utilises the similar heat exchanger geometry and fluid mass flow rates established for Case A. However, the hot stream is modified to simulate the exhaust from an industrial drying installation, characterised as humid air with an inlet temperature of 80°C.

In contrast to the boiler scenario, assessing the thermodynamic performance of a convective dryer introduces a significantly higher degree of complexity. To ensure a rigorous evaluation, the thermodynamic control volume must encompass the entire drying chamber rather than being artificially restricted to the make-up air heater. Consequently, the total thermal demand of the process (Q_{demand}) is overwhelmingly dominated by the latent heat of vaporisation necessary to drive the moisture out of the wet product. By establishing a global mass balance, the moisture evaporation rate ($\dot{m}_{\text{evap}}$) can be deduced from the absolute humidity differential across the system. The comprehensive thermal duty is thus formulated as:

$$Q_{\text{demand}} = [\dot{m}_c c_{p,\text{air}}(T_{\text{target}} - T_{c,\text{in}}) + \dot{m}_{\text{evap}} h_{fg}] \cdot f_{\text{loss}} \tag{11}$$

where $\dot{m}_c$ is the mass flow rate of the dry air, h_{fg} is the enthalpy of vaporisation, and f_{loss} represents a casing heat loss factor. For the investigated industrial scale, accommodating an evaporation rate of approximately $627\,\text{kg/h}$, the true process heat demand equates to approximately $500\,\text{kW}$.

Energetic and exergetic evaluation of the drying process

The conventional First Law efficiency of the system is constrained by the operational efficiency of the gas burner (η_{burner}). By recuperating heat from the moisture-laden exhaust (Q_{rec}), the primary fuel consumption required to satisfy the $500\,\text{kW}$ demand is proportionally reduced:

$$Q_{\text{fuel,after}} = \frac{Q_{\text{demand}} - Q_{\text{rec}}}{\eta_{\text{burner}}} \tag{12}$$

Because the condensing heat exchanger extracts latent heat from the exhaust (energy traditionally considered irrecoverable and falling outside the lower heating value (LHV) boundary of the fuel) the apparent energetic efficiency of the primary fuel input mathematically exceeds 100%. In adherence to academic nomenclature, this metric is redefined as the Energy Utilisation Factor (EUF), analogous to the Coefficient of Performance (COP) in heat pump systems:

$$EUF_{\text{sys}} = \frac{Q_{\text{demand}}}{Q_{\text{fuel,after}}} \cdot 100\% \tag{13}$$

Whilst the First Law analysis quantifies the magnitude of energy savings, the Second Law analysis evaluates the quality of the thermal conversion and locates thermodynamic irreversibilities. In this environment, the useful product exergy ($\dot{B}_P$) is strictly defined by the supply of the total process heat (Q_{demand}) at the specified target temperature (T_{target}), quantified using the Carnot factor:

$$\dot{B}_P = Q_{\text{demand}} \cdot \left(1 - \frac{T_0}{T_{\text{target}}}\right) \tag{14}$$

where T_0 denotes the dead-state ambient temperature. The total exergy input is supplied purely by the chemical exergy of the natural gas ($\dot{B}_F$). The overall exergetic efficiency is then determined as $\eta_{\text{ex,sys}} = \dot{B}_P / \dot{B}_F$.
This exergetic framework isolates the profound, non-linear benefit of low-temperature heat recovery. Although the physical exergy recovered by the H3XA unit is numerically modest, employing it to pre-heat the make-up air partially relieves the primary burner. By displacing a portion of the combustion load, the system successfully prevents the destruction of a disproportionately large amount of high-grade chemical exergy.

2.4. Techno-economic assessment framework

To validate the commercial feasibility of the H3XA module, a Techno-Economic Assessment (TEA) was integrated into the system-level model. The total capital expenditure (CAPEX) is estimated based on the volumetric geometry of the module (number of plates, dimensions, and thickness), the density of the selected material (Stainless Steel 316L, cost: 3.8 EUR/kg), and specific manufacturing and labour cost multipliers.
The annual operational cash flow accounts for the economic value of the avoided fuel consumption (0.07 EUR/kWh CH_4), which is partially offset by the additional electrical secondary loads required to overcome the flow resistance (0.22 EUR/kWh). These secondary loads are calculated based on the hot and cold side pressure drops (ΔP) and the efficiency of the induced draft fans. The economic viability is subsequently evaluated using the Simple Payback Time (SPBT) and the Net Present Value (NPV) projected over the anticipated lifespan of the installation.

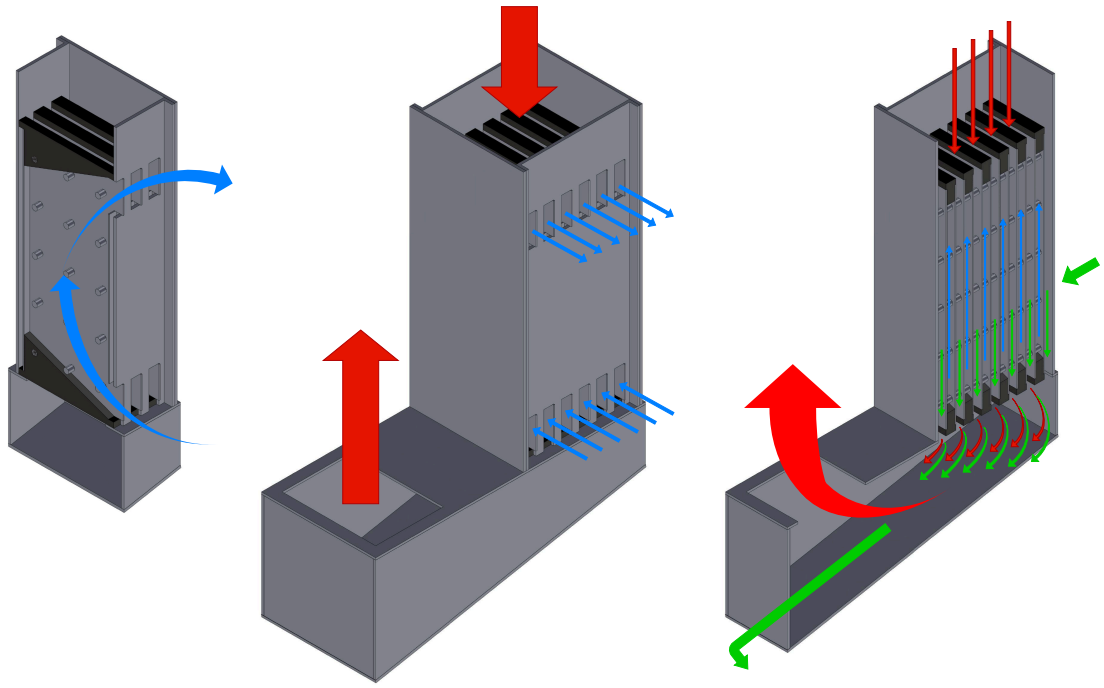

Figure 2: Visualisation of the proposed H3XA design. On the left: Cross-section of the filling plate with the visible flow channel for the cold medium and pins. In the middle: isometric projection. On the right: Cross-section with visible flow channels alternating for cold (blue), hot (red) medium and the third fluid (green; condensate/injection).

3. Results and discussion

3.1. Industrial gas boiler

To provide a comprehensive evaluation of the proposed heat recovery system, the simulation was divided into two distinct operational scenarios. Case A (maximum duty) explores the physical limits of heat recovery for a boiler operating 5,000 hours/year (a standard industrial operating schedule) by utilizing a large-scale heat exchanger. Conversely, Case B (optimal SPBT) prioritizes economic viability and footprint, employing a significantly smaller and better-optimized module. Both configurations utilize Stainless Steel 316L plates with a channel spacing of 6.00 mm, incorporating 8.00 mm diameter spacing pins arranged at 80.00 mm intervals. A visualisation of the proposed HE design can be seen in 2.

3.1.1. Case A: Maximum Duty scenario

The Case A configuration comprises 110 plates, each with a width of 1.00 m and a height of 1.80 m, resulting in a substantial total mass of 1,251.4 kg. As the hot exhaust gas ($\dot{m}$ = 0.2275 kg/s) passes through the exchanger, its temperature is significantly reduced from 140.00°C to 60.66°C. Simultaneously, the cold oxidizer stream (ambient air, $\dot{m}$ = 0.2167 kg/s) is preheated from an inlet temperature of 10.00°C to an impressive 133.75°C.

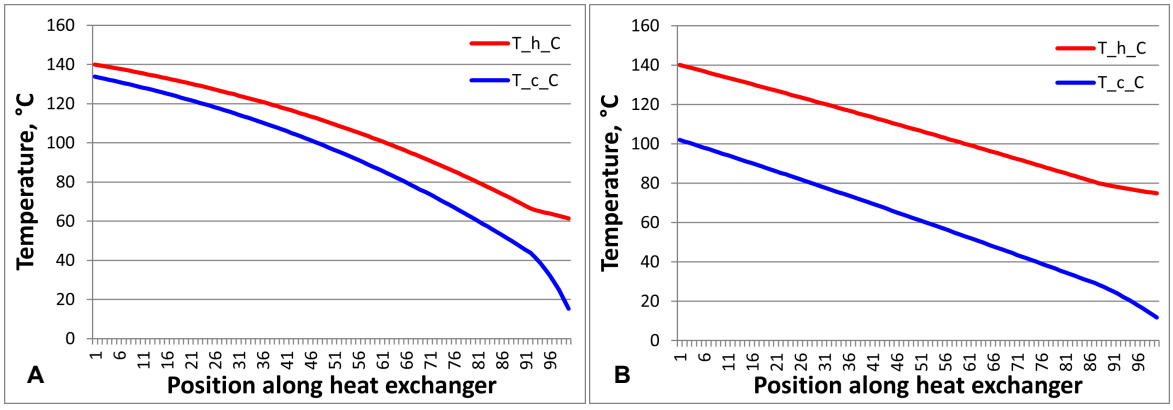

Figure 3: Temperature profiles of the hot exhaust gas and cold oxidizer streams along the H3XA module.

This aggressive heat recovery leads to maximum fuel displacement. By returning this thermal energy to the combustion chamber, the required fuel input is reduced by 5.09%, driving the first-law energetic efficiency of the system up from 94.00% to 99.04%. The resulting Net Cash Flow is maximized at 9,586.77 EUR/year. Despite the high initial CAPEX (15,490.72 EUR) associated with the plate area, the utilization yields a Net Present Value (NPV) of 48,837.29 EUR over 10 years, with a Simple Payback Time (SPBT) of 1.62 years.

3.1.2. Case B: Optimal Payback Time scenario

While Case A proves highly effective, its physical footprint and weight may be impractical for retrofitting standard boiler rooms. Case B represents an economically optimized alternative, comprising 100 smaller plates (0.50 m width by 1.00 m height). This reduces the physical mass by roughly 75%, bringing the estimated exchanger weight down to just 316.0 kg and lowering the CAPEX to 4,016.11 EUR.

In this configuration, the oxidizer is preheated to 101.99°C, and the flue gas exits at a higher temperature of 74.46°C. This still results in a highly respectable first-law efficiency increase to 97.69% and a fuel saving of 3.78%. When evaluated under a standard 5,000 hour operational year, this setup generates 7,110.46 EUR/year in Net Cash Flow. Most importantly, the reduction in material costs results in a faster SPBT of 0.56 years (approximately 7 months), making it a highly attractive investment for typical industrial facilities.

3.1.3. Exergy and Thermodynamic Cost Analysis

While the first-law energy analysis highlights the fuel savings, the extended exergy analysis reveals the qualitative performance of the heat exchangers. Table 1 summarizes the specific exergy (b) and total exergy rates ($\dot{B}$) evaluated against the environmental dead state of 10.00°C and 1.01 bar.

Table 1: Exergy state parameters of the streams before and after modernization.

Stream (state)	$\dot{m}$ [kg/s]	T [°C]	p [bar]	h [kJ/kg]	b [kJ/kg]	$\dot{B}$ [kW]
Before modernization						
Ambient air to boiler (0)	0.2167	10.00	1.010	409.35	0.00	0.00
Flue gas to stack (1)	0.2275	140.00	1.010	692.72	60.60	13.79
After modernization – Case A (max duty)						
Flue gas to ambient (2)	0.2251	60.66	1.010	582.70	35.00	7.88
Preheated air to boiler (3)	0.2167	133.75	1.010	534.26	21.29	4.61
Liquid condensate drain (4)	0.0024	60.66	1.010	253.94	16.98	0.04
After modernization – Case B (optimal SPBT)						
Flue gas to ambient (2)	0.2264	74.46	1.010	610.08	40.03	9.06
Preheated air to boiler (3)	0.2167	101.99	1.010	502.08	12.43	2.69
Liquid condensate drain (4)	0.0011	74.46	1.010	311.74	26.75	0.03

In Case A, the exergy extracted from the flue gas stream amounts to 5.91 kW (13.79 kW - 7.88 kW), with 4.61 kW successfully transferred to the incoming air. This results in an internal exergy destruction (irreversibility) of 1.30 kW within the exchanger. By contrast, the smaller geometry of Case B transfers less total heat and operates with larger mean temperature differences between the streams. Consequently, while only 4.73 kW of exergy is extracted from the flue gas, the exergy destruction within the module is higher (2.04 kW).

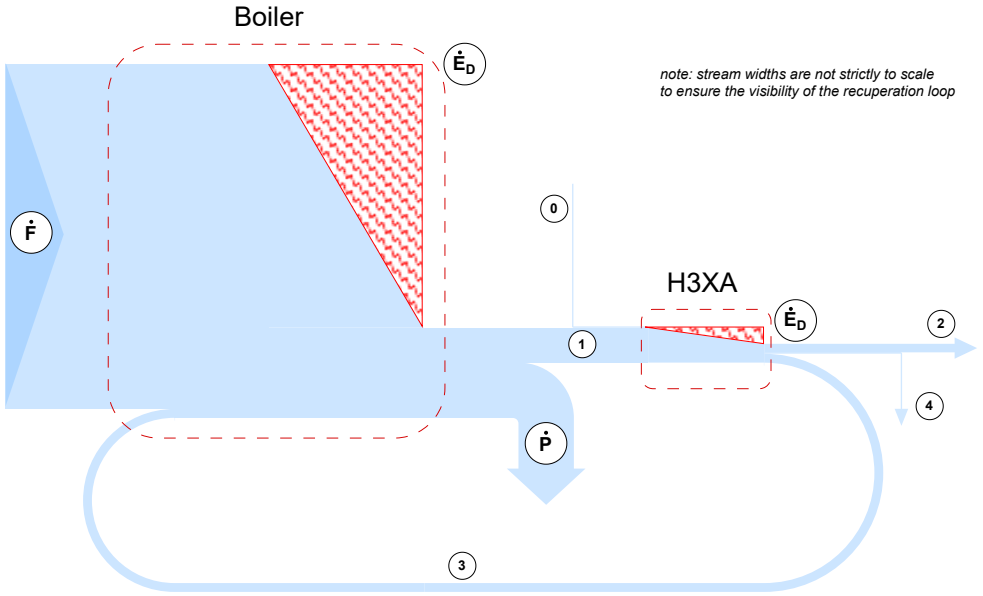

Figure 4: Exergy flow (Grassmann) diagram illustrating the extracted exergy from flue gas, exergy recovered by combustion air, and the associated exergy destruction within the industrial gas boiler system.

Ultimately, both scenarios successfully reduce combustion irreversibilities at the system level. Table 2 presents the global exergy balance of the boiler system. By preheating the oxidizer, the required fuel chemical exergy ($\dot{F}$) is reduced. This elevates the global exergetic efficiency (η_B) of the plant from a baseline of 15.72% to 16.56% (Case A) and 16.34% (Case B).

The comparison of these two scenarios confirms that, while scaling up the heat exchange area yields the highest theoretical thermodynamic recovery, smaller and more economical modules present a very promising commercial viability for standard industrial implementations. A summary of the key performance indicators is presented in Table 3.

Table 2: Global exergy balance of the boiler before and after the integration of the air preheater (H3XA) for both evaluated configurations.

Exergy stream / parameter	Symbol	Before	Case A	Case B
Exergy inputs (resources)				
Fuel chemical exergy	$\dot{F}$	553.19 kW	525.03 kW	532.28 kW
Ambient air inlet (0)	$\dot{B}_0$	0.00 kW	–	–
Preheated air to boiler (3)	$\dot{B}_3$	–	4.61 kW	2.69 kW
Total input	$\sum \dot{B}_{in}$	**553.19 kW**	**529.64 kW**	**534.97 kW**
Exergy outputs (products & exhaust)				
Useful heat to water	$\dot{P}$	86.96 kW	86.96 kW	86.96 kW
Flue gas from boiler (1)	$\dot{B}_1$	13.79 kW	13.79 kW	13.79 kW
Exergy destruction & efficiency				
Exergy destruction in boiler	$\dot{E}_D$	452.44 kW	428.89 kW	434.22 kW
Exergetic efficiency	η_B	15.72%	16.56%	16.34%

Table 3: Comparison of techno-economic and thermodynamic performance indicators for both operational scenarios.

Indicator	Reference (before)	Case A (max duty)	Case B (opt. SPBT)
Operating hours [h/year]	–	5,000	5,000
Exchanger mass [kg]	–	1,251.4	316.0
Energy Utilisation Factor (EUF) [%]	94.00	99.04	97.69
Exergetic efficiency [%]	15.72	16.56	16.34
Fuel saved [%]	–	5.09	3.78
Total CAPEX [EUR]	–	5,490.72	4,016.11
Net Cash Flow [EUR/year]	–	9,586.77	7,110.4
Simple Payback Time [years]	–	1.62	0.56
Net Present Value [EUR]	–	48,837.29	43,695.66

3.2. High-moisture industrial dryer

To assess the heat exchanger's capacity for deep latent heat recovery, similarly to the industrial gas boiler, the simulation evaluated the high-moisture industrial dryer under two distinct scenarios. Unlike the boiler, this application processes significantly higher mass flow rates: the hot, humid exhaust from the drying chamber enters at 3,925 kg/h ($1.0903\,\mathrm{kg/s}$), whilst the cold ambient supply air flows at 3,300 kg/h ($0.9167\,\mathrm{kg/s}$). To accommodate these higher flow rates, both evaluated configurations utilize 150 Stainless Steel 316L plates with an expanded channel spacing of $8.00\,\mathrm{mm}$, incorporating $10.00\,\mathrm{mm}$ diameter spacing pins arranged at $100.00\,\mathrm{mm}$ intervals.

3.2.1. Case A: Maximum duty scenario

The Case A configuration seeks to maximize latent heat extraction by employing substantial heat exchanger dimensions: 150 plates with a width of $1.20\,\mathrm{m}$ and a height of $2.00\,\mathrm{m}$. This expansive geometry results in a total module mass of $2,275.2\,\mathrm{kg}$. As the highly humid exhaust gas ($80.00^\circ\mathrm{C}$) passes through the exchanger, it is deeply cooled to an outlet temperature of $65.79^\circ\mathrm{C}$. Simultaneously, the ambient air stream is preheated from $10.00^\circ\mathrm{C}$ to $71.50^\circ\mathrm{C}$.

The defining characteristic of this configuration is the intense phase change observed within the unit. The condensation rate reaches $0.016\,\mathrm{kg/s}$ (approximately $57.6\,\mathrm{kg/h}$). By recuperating this immense quantity of latent heat, the primary fuel consumption required to satisfy the $500\,\mathrm{kW}$ process demand is reduced by 10.95%. Consequently, the apparent Energy Utilisation Factor (EUF) of the system surges from 98.00% to 110.05%.

Economically, the massive physical footprint results in a high capital expenditure (CAPEX) of 26,162.11 EUR. However, operating at 6,000 hours per year, the intense fuel displacement yields an exceptional Net Cash Flow of 24,571.00 EUR/year. This translates to a Simple Payback Time (SPBT) of just 1.06 years and a commanding Net Present Value (NPV) of 138,711.31 EUR over 10 years.

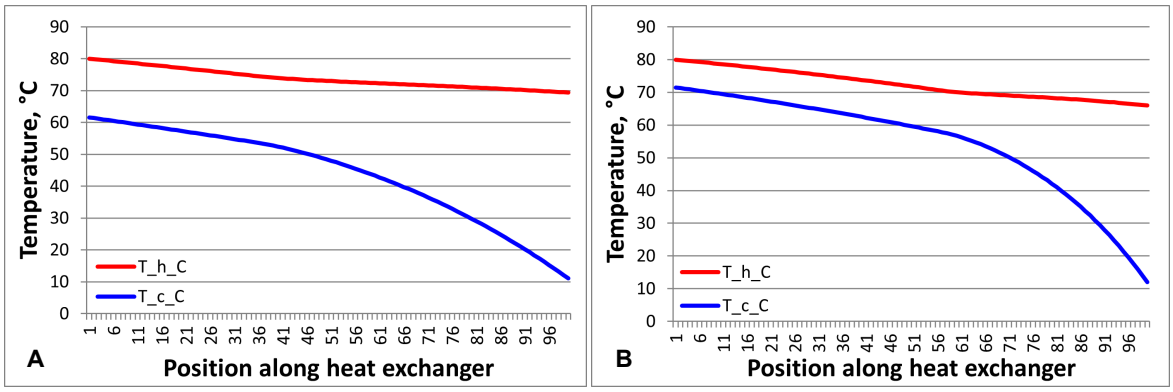

Figure 5: Temperature profiles of the highly humid exhaust gas and cold supply air streams along the H3XA module for the dryer scenario.

3.2.2. Case B: Optimal Payback Time scenario

Recognizing that a > 2.2-tonne module may be structurally prohibitive for certain retrofit applications, Case B presents a financially optimized alternative. This configuration utilizes 150 noticeably smaller plates ($1.00\,\mathrm{m}$ width by $1.20\,\mathrm{m}$ height). The physical mass is halved to $1,137.6\,\mathrm{kg}$, reducing the CAPEX drastically to 13,081.05 EUR.

Despite the reduced surface area, the unit still recovers a substantial amount of latent heat, inducing a condensation rate of $0.014\,\mathrm{kg/s}$ and preheating the incoming oxidizer to $61.56°\mathrm{C}$. The fuel savings remain competitive at 9.18%, elevating the EUF to 107.91%. While the annual Net Cash Flow decreases to 20,607.73 EUR/year, the much lower initial investment results in an exceptionally rapid SPBT of 0.63 years (approximately 7.5 months). The NPV remains remarkably high at 125,198.48 EUR, making this an extremely agile and low-risk industrial investment.

3.2.3. Exergy and thermodynamic cost analysis

The extended exergy analysis, summarized in Table 4, confirms the qualitative superiority of low-temperature latent heat recovery. Evaluated against the environmental dead state of $10.00°\mathrm{C}$ and $1.01\,\mathrm{bar}$, the analysis rigorously isolates the thermodynamic realities of the sub-dew point operations.

Table 4: Exergy state parameters of the streams before and after the integration of the heat exchanger for the drying installation.

Stream (state)	$\dot{m}$ [kg/s]	T [°C]	p [bar]	h [kJ/kg]	b [kJ/kg]	$\dot{B}$ [kW]
Before modernization						
Ambient air to burner (0)	0.9167	10.00	1.010	409.35	0.00	0.00
Flue gas from dryer to stack (1)	1.0903	80.00	1.010	726.43	71.72	78.20
After modernization – Case A (max duty)						
Flue gas to ambient (2)	1.0744	65.79	1.010	681.69	62.46	67.10
Preheated air to burner (3)	0.9167	71.50	1.010	471.28	5.87	5.38
Liquid condensate drain (4)	0.0159	65.79	1.010	275.42	20.38	0.32
After modernization – Case B (optimal SPBT)						
Flue gas to ambient (2)	1.0763	69.27	1.010	689.11	63.89	68.76
Preheated air to burner (3)	0.9167	61.56	1.010	461.26	4.21	3.86
Liquid condensate drain (4)	0.0140	69.27	1.010	290.00	22.84	0.32

The system-level impact of this heat recovery is profoundly non-linear. In Case A, the physical exergy successfully transferred to the incoming air is numerically modest ($\dot{B}_3 = 5.38\,\mathrm{kW}$). However, Table 5 demonstrates that employing this recovered exergy to preheat the supply air displaces a significantly larger portion of the primary combustion load. Specifically, the required chemical fuel exergy ($\dot{F}$) drops from $530.71\,\mathrm{kW}$ to $472.46\,\mathrm{kW}$.

This effect prevents the loss of high-quality chemical exergy in the burner, thereby increasing the overall global exergetic efficiency (η_{sys}) of the drying process, which is elevated from a baseline of 26.36%

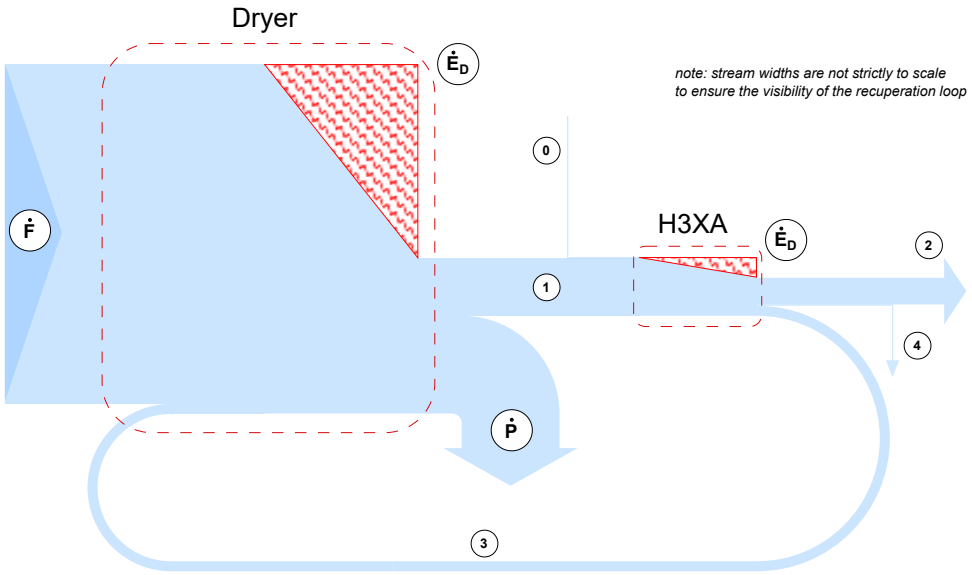

Figure 6: Exergy flow (Grassmann) diagram illustrating the extracted exergy from flue gas, exergy recovered by combustion air, and the associated exergy destruction within the industrial dryer system.

to 29.61% (Case A) and 29.03% (Case B). Consequently, total system irreversibilities ($\dot{E}_D$) are reduced by 53 kW and 45 kW, respectively. A comprehensive summary of the key techno-economic

Table 5: Global exergy balance of the overall drying system before and after modernization.

Exergy stream / parameter	**Symbol**	**Before**	**Case A**	**Case B**
Exergy inputs (resources)				
Fuel chemical exergy	$\dot{F}$	530.71 kW	472.46 kW	481.90 kW
Ambient air inlet (0)	$\dot{B}_0$	0.00 kW	–	–
Preheated air to burner (3)	$\dot{B}_3$	–	5.38 kW	3.86 kW
Total input	$\sum \dot{B}_{in}$	**530.71 kW**	**477.84 kW**	**485.76 kW**
Exergy outputs (products & exhaust)				
Useful exergy to drying air	$\dot{P}$	139.90 kW	139.90 kW	139.90 kW
Flue gas from dryer (1)	$\dot{B}_1$	78.20 kW	78.20 kW	78.20 kW
Exergy destruction & efficiency				
Exergy destruction in dryer system	$\dot{E}_D$	312.61 kW	259.74 kW	267.66 kW
Exergetic efficiency	η_{sys}	26.36%	29.61%	29.03%

Table 6: Comparison of techno-economic and thermodynamic performance indicators for the dryer operational scenarios.

Indicator	**Reference (before)**	**Case A (max duty)**	**Case B (opt. SPBT)**
Operating hours [h/year]	–	6,000	6,000
Exchanger mass [kg]	–	2,275.2	1,137.6
Energy Utilisation Factor (EUF) [%]	98.00	110.05	107.91
Exergetic efficiency [%]	26.36	29.61	29.03
Fuel saved [%]	–	10.95	9.18
Total CAPEX [EUR]	–	26,162.11	13,081.05
Net Cash Flow [EUR/year]	–	24,571.00	20,607.7
Simple Payback Time [years]	–	1.06	0.63
Net Present Value [EUR]	–	138,711.31	125,198.48

and thermodynamic performance indicators for the high-moisture industrial dryer is presented in Table 6.

4. Conclusions

This study presented a comparative energy and exergy analysis of a novel, modular three-fluid heat and mass exchanger (H3XA) designed for low-temperature waste heat recovery. A proprietary 1D

analytical model was employed to evaluate the thermodynamic feasibility of the architecture across two distinct industrial applications: a standard natural gas-fired boiler and a high-moisture industrial drying process. For both applications, the system was evaluated under a Maximum Duty scenario (Case A) and an Optimal Simple Payback Time scenario (Case B). The primary conclusions drawn from the numerical analysis are as follows:

I **Thermo-economic trade-offs in standard boilers:** The integration of the H3XA module proved highly effective in standard combustion systems. While maximizing the heat exchange area (Case A) yielded the highest absolute fuel savings (5.09%) and elevated the first-law energetic efficiency from 94.00% to 99.04%, the smaller, geometrically optimized module (Case B) demonstrated superior commercial viability. By reducing the physical mass of the exchanger by approximately 75%, Case B still achieved a 3.78% fuel reduction while securing an Simple Payback Time (SPBT) of just 0.56 years (approximately 7 months).

II **Thermodynamic quality improvement:** The extended exergy analysis demonstrated that preheating the oxidizer effectively mitigates combustion irreversibility. In the boiler scenario, the global exergetic efficiency of the system improved from a baseline of 15.72% to a peak of 16.56%, verifying that the recovered heat translates into high-quality thermodynamic benefits and a measurable reduction in absolute exergy destruction within the primary burner.

III **Deep latent heat potential and EUF enhancement:** When applied to the high-moisture industrial drying process, the module's operating regime shifted fundamentally to a condensation-dominant phase. Extracting heat from the $80.00^{\circ}\mathrm{C}$ exhaust stream induced intense phase change, achieving a condensation rate of up to $57.6\,\mathrm{kg/h}$ (Case A). This deep latent heat recovery drastically transformed the thermodynamic profile of the system, elevating the overarching Energy Utilisation Factor (EUF) from 98.00% to an apparent 110.05% and driving a robust 10.95% reduction in primary fuel consumption.

IV **Promising thermodynamics and payback times:** The dryer application successfully validated a profound non-linear thermodynamic benefit. By recuperating a numerically modest quantum of physical exergy from the exhaust ($\sim 5.38\,\mathrm{kW}$) and returning it to the burner, the system successfully prevented the destruction of over $58\,\mathrm{kW}$ of high-grade chemical exergy. This multiplier effect elevated the dryer's global exergetic efficiency from 26.36% to 29.61%. Economically, even the bigger module required for Case A yielded an SPBT of just 1.06 years, while the dimensionally optimized Case B achieved payback in 0.63 years, confirming the H3XA design as a financially attractive solution for sub-dew point operations.

While the simulated system integration of H3XA heat exchangers presented in this study reveals strong potential for the proposed technology, it necessitates further empirical research to comprehensively evaluate the associated thermal and flow parameters. To build upon these numerical findings, the next phase of research will focus on the construction and operation of an experimental test rig to validate the 1D analytical model under real-world conditions. Alongside this empirical testing, advanced numerical modeling via Ansys Fluent will be deployed to investigate the internal flow dynamics. A critical objective of these parallel studies will be the implementation of the third-fluid reagent injection, aiming to definitively assess its capability for in-situ corrosion control and exhaust gas scrubbing.

Acknowledgments

This research was financed by the BKM-712/RIE6/2024 08/060/BKM24/1139 project, being part of the statutory research fund of the Silesian University of Technology, Faculty of Power and Environmental Engineering.

Nomenclature

Latin symbols

b	specific physical exergy, $\mathrm{kJ/kg}$
$\dot{B}$	exergy rate, kW
c_p	specific heat capacity at constant pressure, $\mathrm{kJ/(kg \cdot K)}$
$\dot{E}$	exergy transfer or destruction rate, kW
EUF	Energy Utilisation Factor, $\%$
f	empirical or operational factor (e.g., casing heat loss)
h	specific enthalpy, $\mathrm{kJ/kg}$
h_{fg}	specific enthalpy of vaporisation, $\mathrm{kJ/kg}$
H_u	lower heating value (LHV), $\mathrm{kJ/kg}$ or $\mathrm{kJ/m^3}$
M	molar mass, $\mathrm{kg/kmol}$
$\dot{m}$	mass flow rate, $\mathrm{kg/s}$
$\dot{n}$	molar flow rate, $\mathrm{kmol/s}$
p	pressure, bar or Pa
Q	thermal energy or process heat, kW
$\dot{Q}$	heat rate / thermal power, kW
r	specific enthalpy of vaporisation, $\mathrm{kJ/kg}$
s	specific entropy, $\mathrm{kJ/(kg \cdot K)}$
$\dot{S}_{\mathrm{gen}}$	entropy generation rate, $\mathrm{kW/K}$
T	absolute temperature, K or $^{\circ}\mathrm{C}$
x	mole fraction

Greek symbols

α	empirical ratio of chemical exergy to lower heating value
Δ	difference / macroscopic change in a variable
δ	infinitesimal change / denotes destruction or loss rate in exergy balances
η	efficiency, $\%$

Subscripts and superscripts

0	dead state / reference environment
air	oxidiser / air stream
B	boiler / exergetic (efficiency)
burner	gas burner or primary heater
c	carrier gas / dry air stream
ch	chemical (exergy)
D	destruction (exergy)
demand	required process heat demand
evap	evaporated moisture
exhaust	exhaust gas stream
F	fuel
f	physical (exergy)
gen	generation (entropy)
in	inlet conditions
L	external losses (exergy)

loss thermal or casing losses
nom nominal (power)
out outlet conditions
P product
rec recovered / recuperated (heat)
sat saturation state
sys overarching system or global boundary
target target process parameter (e.g., drying temperature)
w water / condensed moisture

References

[1] A. Banasik, W. Kostowski, R. Rolf, M. Figiel, A. Jedynak, and M. Barzantny, "Comparative evaluation of the waste heat potential from selected compressor stations: Natural gas and hydrogen," *Sustainable Energy Technologies and Assessments*, vol. 66, p. 103814, June 2024.

[2] C. Forman, I. K. Muritala, R. Pardemann, and B. Meyer, "Estimating the global waste heat potential," *Renewable and Sustainable Energy Reviews*, vol. 57, pp. 1568–1579, May 2016.

[3] United Nations, "Sustainable Energy for All (SE4All)," 2024. Accessed: 2025-02-20.

[4] European Commission, "Energy Efficiency Directive (EU/2023/1791)," 2023. Accessed: 2025-02-20.

[5] United Nations Climate Change Conference (COP28), "UAE Consensus at COP28," 2023. Accessed: 2025-02-20.

[6] Government of Poland, "Energy Policy of Poland until 2040 (PEP2040)," 2021. Accessed: 2025-02-20.

[7] European Commission. Joint Research Centre., *Defining and accounting for waste heat and cold.* LU: Publications Office, 2021.

[8] Y. Li, S. Ding, Z. Bai, S. Wang, F. Zhang, J. Zhang, D. Xu, and J. Yang, "Corrosion characteristics and mechanisms of typical iron/nickel-based alloys in reductive supercritical water environments containing sulfides," *The Journal of Supercritical Fluids*, vol. 187, p. 105599, Aug. 2022.

[9] M.-J. Li, S.-Z. Tang, F.-l. Wang, Q.-X. Zhao, and W.-Q. Tao, "Gas-side fouling, erosion and corrosion of heat exchangers for middle/low temperature waste heat utilization: A review on simulation and experiment," *Applied Thermal Engineering*, vol. 126, pp. 737–761, Nov. 2017.

[10] A. Politano, "2024 roadmap on membrane desalination technology at the water-energy nexus," *Journal of Physics: Energy*, vol. 6, p. 021502, Apr. 2024.

[11] M. Ugrina and J. Milojković, "Advances in Wastewater Treatment, 2024," *Energies*, vol. 17, p. 1400, Mar. 2024.

[12] B. Sundén and R. M. Manglik, *Plate Heat Exchangers: Design, Applications and Performance*. WIT Press, 2007. Google-Books-ID: P3gTR8YHLHgC.

[13] S. Kakaç, H. Liu, and A. Pramuanjaroenkij, *Heat Exchangers: Selection, Rating, and Thermal Design, Third Edition*. CRC Press, Mar. 2012. Google-Books-ID: sJXpvP6xLZsC.

[14] Y. Wang, J. Jiao, Y. Dai, Z. Ke, Q. Zhao, and F. Li, "Study on heat transfer characteristics of flue gas condensation in narrow gap heat exchangers," *Thermal Science*, vol. 27, no. 6 Part A, pp. 4681–4693, 2023.

[15] R. Mandal, D. S. Ahirwar, and S. Vishwakarma, "Study of plate type heat exchanger with alternative pipe arrangeent using ansys," *International Research Journal of Modernization in Engineering Technology and Science*, vol. 05, pp. 761–788, Nov. 2023.

[16] A. Bahadori, "Estimation of combustion flue gas acid dew point during heat recovery and efficiency gain," *Applied Thermal Engineering*, vol. 31, pp. 1457–1462, June 2011.

[17] Z. Varga and B. Palotai, "Comparison of low temperature waste heat recovery methods," *Energy*, vol. 137, pp. 1286–1292, Oct. 2017.

[18] W. M. Kays and A. L. London, *Compact heat exchangers*. 1984. Publisher: McGraw-Hill, New York, NY.

[19] J. P. Holman, *Heat Transfer Tenth Edition.* McGraw-Hill Education, 2009.

[20] G. Cano and P. Moulin, "Treatment of Boiler Condensate by Ultrafiltration for Reuse," *Membranes*, vol. 12, p. 1285, Dec. 2022.

[21] H. Li and N. Nord, "Transition to the 4th generation district heating - possibilities, bottlenecks, and challenges," *Energy Procedia*, vol. 149, pp. 483–498, Sept. 2018.

[22] Ibragimov, I.I., Indrupskiy, I.M., G. C.A., Khaliullin, T.F., Valiullin, I.V., Zalyatdinov, A.A., Sadreeva, R.Kh., Burlutskiy, E.A., Mingazutdinov, A.N., Remeev, M.M., and Kashapov, I.Kh., "Experimental Assessment of Oil Displacement Efficiency by Flue Gases for a Developed Reservoir in Carbonnate Formation of Urals-Volga Region," *Georesursy*, vol. 26, no. 1, pp. 127–135, 2024.

[23] O. Farhat, J. Faraj, F. Hachem, C. Castelain, and M. Khaled, "A recent review on waste heat recovery methodologies and applications: Comprehensive review, critical analysis and potential recommendations," *Cleaner Engineering and Technology*, vol. 6, p. 100387, Feb. 2022.

[24] R. K. Srivastava and W. Jozewicz, "Flue Gas Desulfurization: The State of the Art," *Journal of the Air & Waste Management Association*, vol. 51, pp. 1676–1688, Dec. 2001.

[25] P. Ostrowski, M. Pronobis, and F. Szelejewski, "EWHR technology for heat recovery and reduction of emissions in boilers," *Rynek Energii*, vol. 2021, no. 6, pp. 28–35, 2021.

[26] The Polish Patent Office, "PL 244733 Method of reducing gaseous pollutants in process gases, especially reduction in exhaust gases from heating and industrial boiler rooms," 2022.

[27] The Polish Patent Office, "PL 246408 Plate heat exchanger for low-pressure gaseous media, especially those with similar specific heat capacity," 2024.